processes

MDPI

Article

Coleus aromaticus Ethanolic Leaves Extract Mediates Inhibition of NF-κB Signaling Pathway in Lung Adenocarcinoma A549 Cells

Gehad Subaiea [1,*], Ahmed Alafnan [1], Abdulwahab Alamri [1], Talib Hussain [1,2], Shimaa Mahmoud Hassoun [1], Amr Selim Abu Lila [3,4], El-Sayed Khafagy [5,6] and Ahmed A. Katamesh [4,7]

1 Department of Pharmacology and Toxicology, College of Pharmacy, University of Ha'il, Ha'il 81442, Saudi Arabia
2 Lucknow Vision Institute of Health Sciences, Lucknow 226020, India
3 Department of Pharmaceutics and Industrial Pharmacy, Faculty of Pharmacy, Zagazig University, Zagazig 44519, Egypt
4 Department of Pharmaceutics, College of Pharmacy, University of Ha'il, Ha'il 81442, Saudi Arabia
5 Department of Pharmaceutics, College of Pharmacy, Prince Sattam Bin Abdulaziz University, Al-Kharj 11942, Saudi Arabia
6 Department of Pharmaceutics and Industrial Pharmacy, Faculty of Pharmacy, Suez Canal University, Ismailia 41522, Egypt
7 Department of Pharmaceutics, Central Administration of Drug Control, Egyptian Drug Authority "EDA", Giza 11553, Egypt
* Correspondence: g.subaiea@uoh.edu.sa

Abstract: Lung cancer is the second leading cause of cancer-related mortalities globally. Failure in diagnosis at early stages and limited effective chemotherapeutics has severely impeded the clinical management of patients suffering from lung carcinoma. At present, researchers across the world are focused on exploring biologically active natural products for treating various cancers, which can thus be further investigated for their chemotherapeutical potential. *Coleus aromaticus* is a common herb used in culinary practices and has previously been shown to possess various medicinal characteristics. In the present study, the anti-cancer effects of ethanolic extract of *C. aromaticus* leaves (EtOH-LCa) against non-small cell lung carcinoma (NSCLC) A549 cells were screened. It was observed that EtOH-LCa reduced the viability of A549 cells and obstructed the cell cycle progression in a concentration-dependent manner. Importantly, EtOH-LCa succeeded in instigating the production of reactive oxygen species (ROS) ($p < 0.001$) within A549 cells. The elevation in ROS levels was concomitantly followed by the disruption of nuclear morphology and the loss in mitochondria viability within A549 cells. In addition, EtOH-LCa was successful in increasing the activity of caspases-3, which further aided in increasing apoptosis. Most importantly, EtOH-LCa decreased NF-κB expression ($p < 0.05$) along with modulating mRNA expression of pro-/anti-apoptotic genes; Bax, Bad, Bcl-2 and Bcl-X_L within NSCLC A549 cells. Collectively, it could be concluded that EtOH-LCa possessed considerable anti-cancer effects against NSCLC A549 cells; however, further molecular studies are warranted to completely establish the chemotherapeutical potential of EtOH-LCa.

Keywords: A549; apoptosis; *Coleus aromaticus* extract; NF-κB; non-small cell lung carcinoma; ROS

Citation: Subaiea, G.; Alafnan, A.; Alamri, A.; Hussain, T.; Hassoun, S.M.; Lila, A.S.A.; Khafagy, E.-S.; Katamesh, A.A. *Coleus aromaticus* Ethanolic Leaves Extract Mediates Inhibition of NF-κB Signaling Pathway in Lung Adenocarcinoma A549 Cells. *Processes* **2023**, *11*, 1332. https://doi.org/10.3390/pr11051332

Academic Editors: Bonglee Kim, Maria das Graças Almeida, Jorge A. López and Jefferson Romáryo Duarte Da Luz

Received: 16 March 2023
Revised: 7 April 2023
Accepted: 22 April 2023
Published: 26 April 2023

1. Introduction

Lung cancer is considered the prime cause behind high cancer-related deaths globally. In accordance with the recent global cancer observatory report, 2,206,771 new diagnoses of lung cancer were confirmed, which constituted 11.4% of all the diagnosed cancer cases in 2021. Furthermore, lung cancer was also attributed as the main cause behind 18% of all the 9,958,133 deaths that occurred because of different cancers in 2021 [1]. Based on histopathological evidence, lung cancer is classified as either Non-Small Cell Lung

Carcinoma (NSCLC) or Small Cell Lung Carcinoma (SCLC) [2]. It has also now been recognized that most diagnosed cases of lung cancer fall under NSCLC, whereas the others resemble the characteristic attributes of SCLC or resemble the features of both NSCLC as well as SCLC [3]. During the initial advent of chemotherapeutic usage, clinical care for lung carcinomas was dependent upon the usage of methotrexate and doxorubicin; however, their therapeutic effects were minimal. Nevertheless, with subsequent advancements in chemotherapeutics, such as taxanes, vinorelbine and gemcitabine, they were further used for treating patients with lung carcinomas [4].

Currently, researchers across the globe are focusing on evaluating the usage of novel complementary therapeutics having the potential of aiding the clinical management of different ailments including various cancers [5]. Since ancient times, the consumption of plant-based products has been part of conventional remedies by ethnic groups around the world [6]. Intriguingly, these plant-derived products are documented for their medicinal and anticancer attributes and are involved primarily in modulating various pathways regulating cellular development, proliferation, and apoptosis [7]. *Coleus aromaticus* is a medicinally important herb of the *Lamiaceae* family belonging to the *Plectranthus* genus, which is usually referred to as Indian borage. *C. aromaticus* is primarily a succulent aromatic herb that is perineal and grows in 30–90 cm tall bushes throughout India [8]. Previous reports have documented the presence of more than 50 bioactive volatile and 30 non-volatile compounds within different parts of the *C. aromaticus* plant [8,9]. These bioactive constituents fall under the category of flavonoids, catechol, alkaloids, terpenoids, sterols, terpenes, glycosides, tannins, phenol, and lactone [8,9]. These diverse active constituents bestow the *C. aromaticus* plants with a broad spectrum of activities; *C. aromaticus* plants are commonly used as a conventional remedy for chronic asthma, malarial fever, helminthiasis, epilepsy, and bronchitis [8,10,11]. Nevertheless, so far only a few limited reports have been published that have elucidated the anticancer effects of *C. aromaticus* against cervical and breast cancer cells [12,13].

NF-κB-mediated signaling has been studied extensively with special emphasis on the initiation and progression of cancer. NF-κB signaling constituents have also been reported to play key role in the progression of different malignancies including breast, colon, and rectal cancers [14,15]. In vitro and in vivo studies have also shown significant linkage between the carcinogenesis of lung cancer and NF-κB signaling [16–18]. It is now clear that chronic activation of NF-κB signaling in myeloid cells plays a primitive role in promoting the progression of lung cancer by inducing an inflammatory tumor microenvironment [9]. Impeding the chronic expression of NF-κB signaling has also been linked to the activation of apoptosis in cancer cells along with concomitant reduction with the invasiveness and proliferation potential of cancer cells which further increases their sensitivity to chemotherapeutics [19,20].

In this study, we evaluated the anticancer potential of EtOH-LCa on lung cancer A549 cells by examining its effects on cell viability, apoptosis induction, ROS levels, and mitochondrial function. Finally, the role of EtOH-LCa in regulating the NF-κB signaling pathway in A549 cells was also investigated.

2. Materials and Methods

2.1. Materials

3-(4,5-dimethylthiazol-2-yl)-2,5-diphenyl tetrazolium bromide (MTT), Rhodamine-123 (Rh-123) and 2′, 7′-Dichlorofluorescin diacetate (DCF-DA) stain were procured from Himedia (Maharashtra, India). Consumables required specifically for maintaining the cell culture such as Dulbecco's Modified Eagle Medium (DMEM), fetal bovine serum (FBS), along with antibiotic–antimycotic solution were procured from Gibco (Gaithersburg, MD, USA). Propidium iodide was purchased from Sigma Aldrich, St. Louis, MO, USA. Human-specific NF-κB ELISA Kit (Cat No. ab176648) was procured from Abcam (Cambridge, UK), whereas a caspase-3 colorimetric assay kit was procured from BioVision (Waltham, MA, USA).

2.2. Cell Culture

Human-derived non-small cell lung carcinoma A549 cells were obtained from National Center of Cell Sciences (Maharashtra, India). The cells were proliferated in an ambient tissue culture environment consisting of humidified air with CO_2 (5%) at 37 °C. The cells were cultured in DMEM and nourished with 10% FBS and 1% antibiotic-antimycotic solution. Phase contrast and fluorescence imaging reported in this study were done using an FLoid imaging station (Thermo-Fisher Scientific, Waltham, MA, USA).

2.3. Plant Sample and Authentication

The leaves of *Coleus aromaticus* plants with the twigs attached were acquired non-commercially from the Garden of Integral University, identified properly, and deposited to the institutional herbarium for accession number (IU/PHAR/HRB/22/06).

2.4. Coleus Aromaticus Extract Preparation

The leaves of the *Coleus aromaticus* plant were cleaned with running water and were subsequently crushed through a pestle and mortar by adding liquefied nitrogen. The powdered leaf was then wrapped carefully in a muslin cloth and loaded into a Soxhlet apparatus. The extraction process was undertaken in analytical grade ethanol at controlled temperatures fluctuating between 78–80 °C for approximately 5 h. Thereafter, the obtained extract was filtered twice, and the solvent was allowed to evaporate under a vacuum. Eventually, the dried ethanolic extract obtained from the leaves of the *Coleus aromaticus* plant (EtOH-LCa) was collected in sterile Eppendorf tubes that were stored at 4 °C until further use.

2.5. GC-MS Analysis

Identification of phytocompounds within EtOH-LCa was accomplished through GC-MS as per the protocol described previously [21]. Prior to its estimation, the extract was solubilized in ethanol (100% *v/v*) and analyzed through Ultra-Mass Spectrometer (Shimadzu QP 2010, Tokyo, Japan) using an RTXi-5MS column. The parameters followed during the analysis have been mentioned in Table 1. An injector was initially used for administering the sample into the instrument in the presence of He through split mode. The retention time of screened phytochemicals along with their pattern of fragmentation was used for their identification of the same using the NIST11.0 spectral library and aided subsequently by the GC-MS Real-Time Analysis Software version 1.10 beta.

Table 1. Set parameters followed for GC-MS-based estimation of phytoconstituents.

Parameters	Range
Ion source temperature	200 °C
Column flow rate	1.24 mL/min
Column oven temperature	280 °C
Column injector temperature	250 °C
Pressure mode	66.7 kPa
Total flow rate	10.4 mL/min
Interface temperature	260 °C

2.6. Assessment of EtOH-LCa-Mediated Cytotoxicity

Cytotoxicity induced by EtOH-LCa, against A549 cells, was estimated by a tetrazolium dye-based assay as described previously [22]. The assay was initiated by exposing 1×10^4 A549 cells to varying concentrations of EtOH-LCa ranging from 0 to 200 µg/mL for 24 h in a sterile cell culture environment. After the incubation was over, the cells were treated with 100 µL MTT dye (5 µg/µL) for an additional 4 h. Subsequently, the cells were supplemented with 100 µL of DMSO and the plate was subjected to gentle shaking at 37 °C for around 30 min in darkness, since the MTT reagent is sensitive to light. Finally, the

amount of solubilized formazan crystal was quantified spectrophotometrically at 570 nm. The cell viability was then expressed using the following formula.

$$Cell\ viability\ (\%) = \frac{Absorbance\ of\ treated\ cells}{Absorbance\ of\ untreated\ cells} \times 100 \quad (1)$$

2.7. Assessment of EtOH-LCa Mediated Effects on Morphology

The effect of EtOH-LCa in disrupting the morphology of A549 cells was evaluated using phase contrast microscopy. As stated above, a similar number of cells was exposed to varying concentrations of EtOH-LCa (10, 20 and 30 μg/mL) for 24 h in a sterile cell culture environment. Subsequently, the cells belonging to different treatment groups and untreated control were visualized and respective photomicrographs were taken. The alterations within morphological attributes were compared to untreated A549 control cells.

2.8. EtOH-LCa-Mediated Effects on Nuclear Morphology

The potential of EtOH-LCa to alter the nuclear morphology of A549 cells was qualitatively evaluated using Hoechst-33342 stain [22], and 1×10^4 A549 cells were exposed to the above-stated concentration of EtOH-LCa for 12 h under optimum culture conditions. After incubation, the media from each well of different groups was decanted and was replaced with Hoechst-33342 for 30 min. Finally, the wells were washed using PBS to remove any excess stain and the photomicrographs were captured and assessed qualitatively in comparison with the untreated control through a fluorescence microscope.

2.9. Assessment of EtOH-LCa Mediated Effects on Caspase-3 Activity

A colorimetric kit specific for caspase-3 activity was also used during the study. Briefly, 1×10^6 A549 cells were exposed to the stated concentrations of EtOH-LCa for 24 h under standard cell culture conditions. Next, the cells were lysed using 50 μL of a chilled PBS buffer. The suspension was centrifuged for 1 min at 10,000 rpm and the resultant supernatant was immediately placed on ice. After quantification of the protein in the lysate, re-dilution of the lysate was done in 50 μL of chilled lysis buffer. Thereafter, the cell lysate was supplemented to a 96-well plate, in which each well was pre-coated with 10 mM dithiothreitol (DTT) and was further followed by the addition of 4 mM DEVD-pNA. The plate was then incubated at 37 °C for 1 h. After incubation, the absorbance of each well was recorded at 405 nm and the results were expressed as a change in activity percentage by making comparisons with the control group.

To evaluate the impact of caspase inhibitors on cell viability, A549 cells were pretreated with a caspase-3 inhibitor (Z-DEVD-FMK; 50 μM) for 2 h. After 24 h of EtOH-LCa treatment, cell viability was determined using the MTT test.

2.10. Evaluation of EtOH-LCa Mediated Effects on Intracellular ROS

To gain an insight into the impact of EtOH-LCa on cellular oxidative stress, DCFH-DA-based detection of reactive oxygen species (ROS) was done both qualitatively and quantitatively as per the methods stated elsewhere [23]. For qualitatively assessing the efficacy of EtOH-LCa in modulating intracellular ROS level, 1×10^4 A549 cells were treated with the stated concentration of EtOH-LCa and were further incubated under optimum culture conditions for 12 h. Subsequently, media in each well was supplemented with 10 μM DCFH-DA and the plate was re-incubated at 37 °C for 30 min. Finally, the cells were washed using 1X PBS and were then visualized for their DCF-DA mediated fluorescence through a fluorescence microscope.

During the quantitative evaluation, 1×10^5 A549 cells were treated and incubated with EtOH-LCa and DCFH-DA as stated for qualitative assessment. Both treated and untreated A549 cells were then pelleted for 2 min at 1500 rpm and 37 °C. The pellet obtained from different groups was then resuspended in 10 μM DCFH-DA for 30 min in darkness at 37 °C. The absorbance of DCF-DA in each group was then recorded through a hybrid multi-mode

microplate reader (Synergy H1, BioTek, VT, USA). Interpolation of the results was done in terms of the percentage of DCF-DA mediated fluorescence intensity in comparison with control A549 cells.

2.11. Assessment of EtOH-LCa Mediated Effects on Mitochondrial Membrane Potential ($\Delta\Psi m$)

The viability of A549 mitochondria was also evaluated using mitochondrial potential sensitive Rhodamine (Rh)-123 stain as published previously. Initially, 1×10^4 A549 cells were subjected to treatment with stated concentrations of EtOH-LCa for 12 h. Thereafter, the cells were re-treated with 5 µg/µL of Rh-123 followed by a brief incubation of 30 min in darkness at 37 °C. The cells were eventually washed gently and then were visualized and the photomicrographs were captured using a fluorescence microscope.

2.12. Cell Cycle Assay

To investigate the effect of EtOH-LCa on cell cycle regulation, A549 cells were analysed by flow cytometry using the DNA intercalating fluorochrome PI [24]. Shortly after, 5×10^5 cells were seeded and cultured overnight in a six-well plate. Subsequently, cells were treated with various concentrations of EtOH-LCa for an additional 24 h. Then, the cells were centrifuged at 500 rpm for 5 min followed by the addition of RNase A (50 µg/mL) and incubated further for 30 min at room temperature. This was followed by the fixation of treated cells with ice-cold ethanol. Finally, PI (25 µg/mL) was added in each well followed by incubation at room temperature for 30 min. The cell cycle analysis was performed using FACS Calibur (BD Biosciences, San Diego, CA, USA).

2.13. Assessment of EtOH-LCa Mediated Effects on NF-κB Levels

The EtOH-LCa-mediated modulatory effect of NF-κB levels in A549 cells was also evaluated. NF-κB/p65 levels in EtOH-LCa treated and/or untreated control cells were estimated by the anti-human NF-κB/p65 colorimetric ELISA kit.

2.14. qRT-PCR-Based Assessment of Gene Expression

Approximately 1×10^6 A549 cells were treated with the above stated concentration of EtOH-LCa under optimum cell culture conditions for 24 h. Post-incubation, RNA was isolated from cells of different treated and/or untreated groups using the Miniprep purification kit (Himedia, Pune, India). Subsequently, 2 µg of isolated RNA was used for cDNA synthesis through a commercially available kit (Thermo-Fisher Scientific, Waltham, MA, USA). The primers employed for the synthesis of cDNA are stated in Table 2. The samples were then analyzed through qPCR using a commercially available SYBR Green qPCR kit (Thermo-Fisher Scientific, Waltham, MA, USA). The GAPDH gene was used for normalization and the observations were analyzed by a comparative CT method. The results were expressed as a fold change through the $^{2\Delta\Delta}$CT method.

Table 2. Sequences of primers.

Gene Name	Forward Sequence	Reverse Sequence
GAPDH	CGACCACTTTGTCAAGCTCA	CCCCTCTTCAAGGGGTCTAC
Bcl2	ATTGGGAAGTTTCAAATCAGC	TGCATTCTTGGACGAGGG
Bax	TCAGGATGCGTCCACCAAGAAG	TGTGTCCACGGCGGCAATCATC
Bad	CCTCAGGCCTATGCAAAAAG	AAACCCAAAACTTCCGATGG
Bcl-X_L	GCCACTTACCTGAATGACCACC	AACCAGCGGTTGAAGCGTTCCT

2.15. Statistical Analysis

All numerical data are presented as mean ± SEM of three independent experiments. Comparisons between the mean of different groups were done with one-way ANOVA (Dunnett's multiple comparisons post-hoc tests). Statistical significance between groups was considered when * $p < 0.05$, ** $p < 0.01$, and *** $p < 0.001$.

3. Results

3.1. Identification of Various Phytoconstituent

GC-MS-based characterization of EtOH-LCa was adopted to identify the bioactive constituents of the extract (Figure 1). Characterization of EtOH-LCa showed the presence of various phytoconstituents including phytol, 1-hexadecanol, 2-propenoic acid, 3-(4-methoxyphenyl)-, 2-ethylhexyl ester, phytyl stearate, lathosterol, stigmasterol, alpha-amyrin and quebrachamine A total of 40 phytoconstituents were identified that have been listed in Table 3.

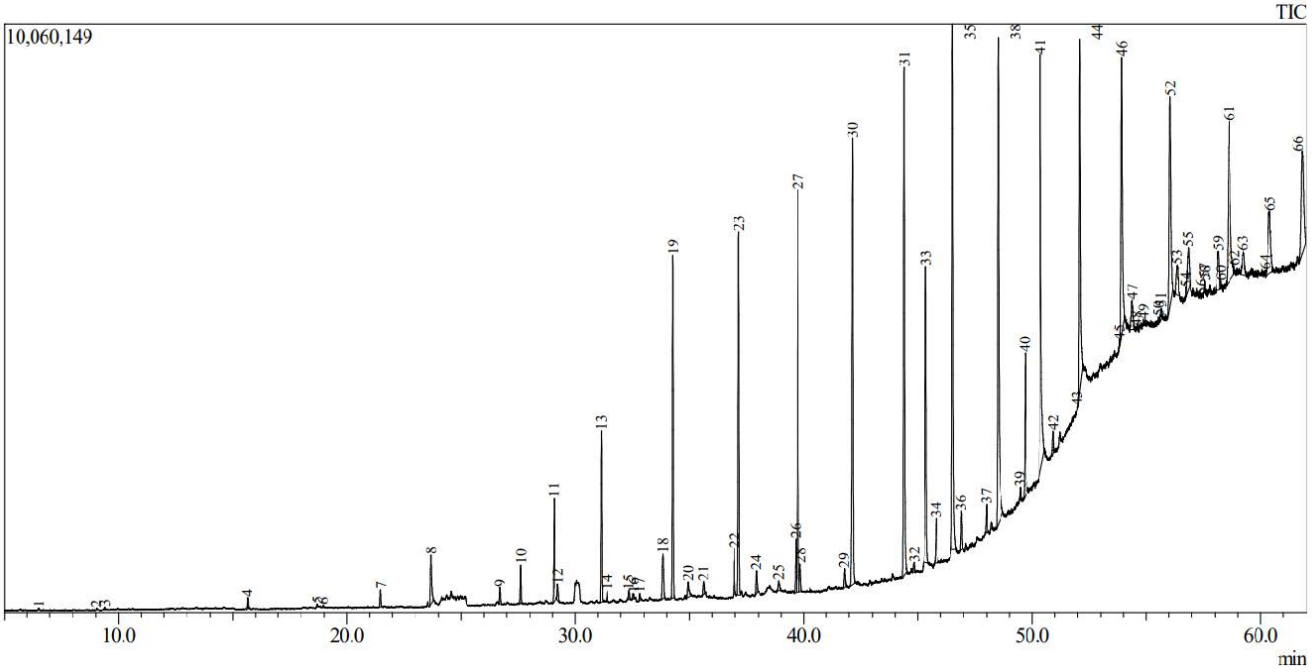

Figure 1. Chromatogram obtained from the GC/MS with the extract of *Coleus aromaticus* leaves.

Table 3. Shows the components identified in ethanolic extract of *Coleus aromaticus* leaves.

S. No.	Retention Time	Area (%)	Compound Name	Molecular Formula
1.	6.504	0.02	2-Methylcyclopentanol	$C_6H_{12}O$
2.	9.398	0.03	1-Decene	$C_{10}H_{20}$
3.	15.650	0.10	1-Dodecanol	$C_{12}H_{26}O$
4.	18.707	0.04	Phenol, 5-methyl-2-(1-methylethyl)-, acetate	$C_{12}H_{16}O$
5.	18.957	0.03	1H-3a,7-Methanoazulene	$C_{11}H_{10}$
6.	21.472	0.20	1-Tetradecanol	$C_{14}H_{30}O$
7.	23.689	0.85	1-Dodecanol	$C_{12}H_{26}O$
8.	26.695	0.21	1-Hexadecanol	$C_{16}H_{34}O$
9.	27.615	0.45	Hexadecamethylcyclooctasiloxane	$C_{16}H_{48}O_8Si_8$
10.	29.070	1.33	n-Tridecan-1-ol	$C_{13}H_{28}O$
11.	29.231	0.24	Propanoic acid	$C_3H_6O_2$
12.	31.142	2.03	Octadecamethylcyclononasiloxane	$C_{18}H_{54}O_9Si_9$
13.	31.387	0.12	Behenic alcohol	$C_{22}H_{46}O$
14.	32.335	0.12	6-Octen-1-ol, 3,7-dimethyl-, propanoate	$C_{13}H_{24}O_2$
15.	32.816	0.10	1,2-Benzenedicarboxylic acid, bis(2-methylpropyl) ester	$C_{16}H_{22}O$
16.	33.838	0.79	Cyclodecasiloxane, eicosamethyl-	$C_{20}H_{60}O_{10}Si_{10}$
17.	34.947	0.33	n-Hexadecanoic acid	$C_{16}H_{32}O_2$
18.	35.619	0.20	Irganox 1076 TMS	$C_{38}H_{70}O_3Si$
19.	37.921	0.33	Phytol	$C_{20}H_{40}O$
20.	38.907	0.17	2-Propenoic acid, 3-(4-methoxyphenyl)-, 2-ethylhexyl ester	$C_{18}H_{26}O_3$

Table 3. *Cont.*

S. No.	Retention Time	Area (%)	Compound Name	Molecular Formula
21.	39.844	0.38	Phytyl stearate	$C_{38}H_{74}O_2$
22.	44.396	7.28	Tetracosamethyl-cyclododecasiloxane	$C_{24}H_{72}O_{12}Si_{12}$
23.	44.848	0.13	Tetrapentacontane	$C_{54}H_{110}$
24.	45.344	4.45	Bis(2-ethylhexyl) phthalate	$C_{24}H_{38}O_4$
25.	45.796	0.63	4,4′-Methylenebis(2,6-DI-tert-butylphenol)	$C_{29}H_{44}O_2$
26.	46.887	0.51	Linalyl isobutyrate	$C_{14}H_{24}O_2$
27.	49.486	0.15	Hexacontane	$C_{60}H_{122}$
28.	49.699	2.07	4-Hydroxy-7,7′,8,8′,11,11′,12,12′,15,15′-decahydro-beta, psi-carotene	$C_{40}H_{66}O$
29.	50.935	0.31	Tetracosane	
30.	51.967	0.04	2,6-Dichloro-4-nitrophenol	$C_6H_3Cl_2NO_3$
31.	53.823	0.08	Oxirane, hexadecyl	$C_{18}H_{36}O$
32.	54.382	0.65	α-Tocopherol-β-D-mannoside	$C_{24}H_{50}$
33.	56.341	0.78	Lathosterol	$C_{27}H_{46}O$
34.	56.730	0.06	Profenofos	$C_{11}H_{15}BrClO_3PS$
35.	56.841	1.16	Stigmasterol	$C_{29}H_{48}O$
36.	57.403	0.04	Quebrachamine	$C_{19}H_{26}N_2$
37.	57.537	0.12	Octanedioic acid dimethyl ester	$C_{10}H_{18}O_4$
38.	58.257	0.07	Testosterone decanoate	$C_{29}H_{46}O_3$
39.	59.219	0.84	Alpha-amyrin	$C_{30}H_{50}O$
40.	60.220	0.02	Monocrotophos	$C_7H_{14}NO_5P$

3.2. EtOH-LCa Exerts Cytotoxic Effects in Lung Carcinoma Cells

MTT assay was adopted to assess the cytotoxic effect of various concentrations of EtOH-LCa against A549 cells. As demonstrated in Figure 2A, EtOH-LCa suppressed the proliferation of A549 cells in a concentration-dependent manner. We found that EtOH-LCa reduced the viability of A549 cells to 73.46 ± 3.19%, 52.42 ± 4.53% and 24.73 ± 3.94%, at the suggested concentrations of 10, 20 and 30 µg/mL, respectively (Figure 2A). The calculated IC50 value of EtOH-LCa against A549 was 15.44 ± 1.07 µg/mL. Collectively, treatment with EtOH-LCa could efficiently suppress the growth of lung cancer cells in a concentration-dependent manner.

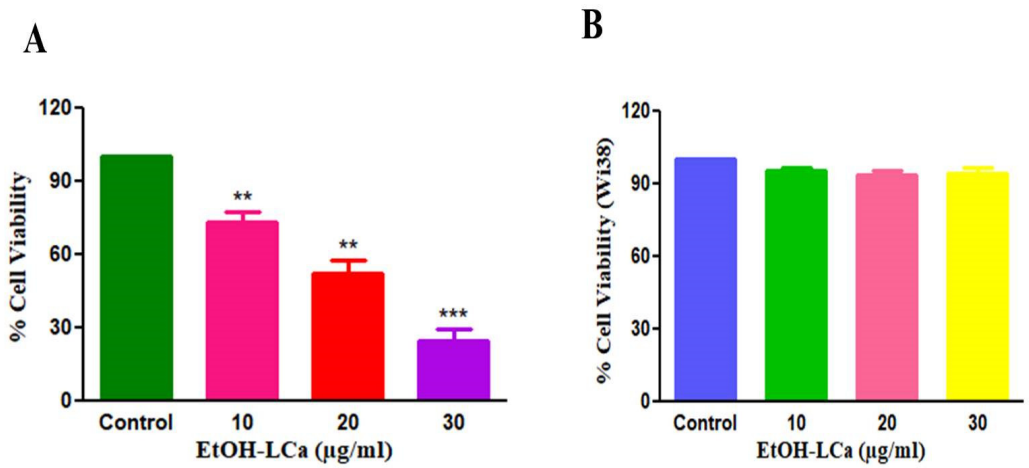

Figure 2. EtOH-LCa-mediated cytotoxic effects against (**A**) A549 lung cancer cells; and (**B**) normal human lung fibroblast Wi38 cells, as assessed by MTT assay after 24 h of exposure. Data reported include mean ± SEM of three separate experiments. Significance among different dosage groups was determined using one-way ANOVA followed by Dunnett post-hoc test. ** $p < 0.01$ and *** $p < 0.001$.

In addition, the cytotoxic potential of EtOH-LCa was examined against noncancerous cells via MTT assay. Intriguingly, EtOH-LCa failed to exert any cytotoxic effects on normal human lung fibroblast Wi-38 cells as assessed by MTT assay (Figure 2B).

3.3. EtOH-LCa Induces Significant Morphological Aberrations in Lung Carcinoma Cells

Phase-contrast microscopy was utilized to trace the possible morphological alterations in A549 upon treatment with EtOH-LCa (Figure 3). The photomicrographs demonstrated that untreated or control cells maintained their flattened morphology, whereas the EtOH-LCa -treated cells exhibited multiple alterations such as rounding up of cells, reduced cell count and withering of cell organelles. These findings suggest that treatment with various concentrations of EtOH-LCa induces substantial morphological alterations within A549 lung carcinoma cells.

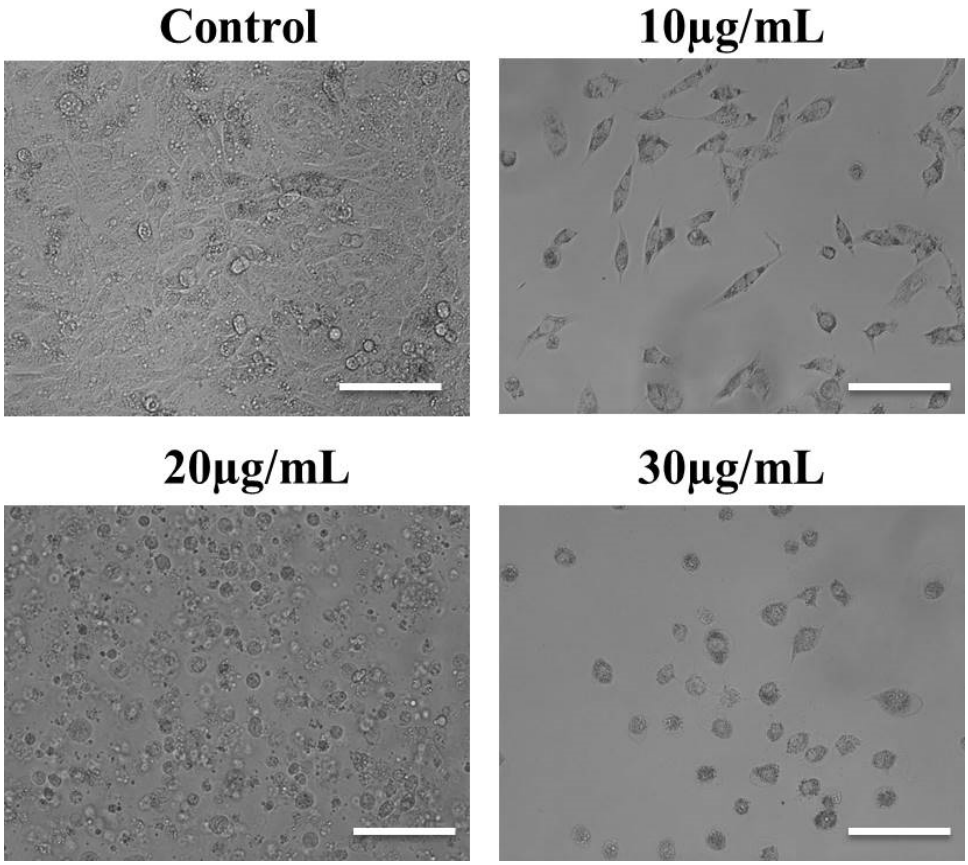

Figure 3. Morphological alterations within the A549 cells after treatment with various concentrations of EtOH-LCa for 24 h. Magnification: 20×; Scale bar = 100 µm.

3.4. EtOH-LCa Generates High ROS -Mediated Oxidative Stress in Lung Carcinoma Cells

The effect of EtOH-LCa treatment on ROS-mediated oxidative stress was studied by performing DCFH-DA staining. As demonstrated in Figure 4A, significantly high levels of ROS, as manifested by higher fluorescence intensity, were observed in A549 cells treated with EtOH-LCa, compared to the untreated or control cells. In addition, EtOH-LCa triggered the production of ROS in a concentration-dependent manner; significantly higher fluorescence intensities were observed in cells treated with 30 µg/mL EtOH-LCa compared to that in cells treated with either 10 µg/mL or 20 µg/mL EtOH-LCa, respectively (Figure 4B). These findings implicated that EtOH-LCa produces substantial ROS in lung cancer cells.

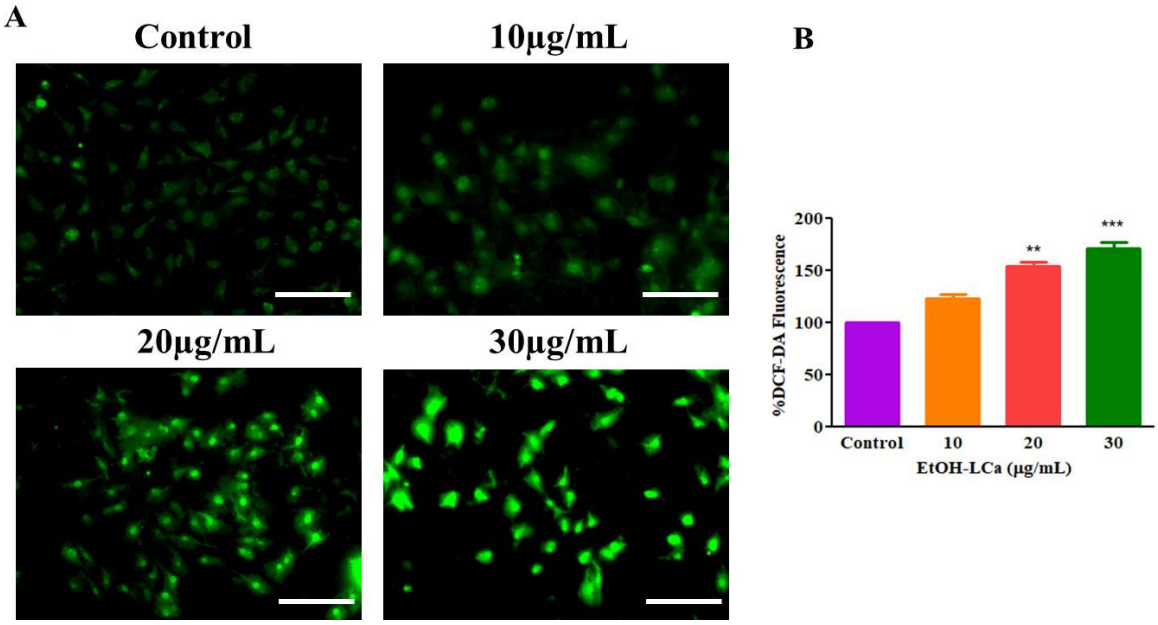

Figure 4. (**A**) EtOH-LCa-mediated effects on the instigation of intracellular ROS within human lung cancer A549 cells. (**B**) Quantification of augmented ROS in A549 cells after treatment with EtOH-LCa. Scale bar = 100 µm, Magnification: 20×. ** $p < 0.01$ and *** $p < 0.001$. Data reported include mean ± SEM. ** $p < 0.01$ and *** $p < 0.001$ vs. untreated control.

3.5. EtOH-LCa Induces Nuclear Condensation and Fragmentation in Lung Carcinoma Cells

DAPI staining was performed to study EtOH-LCa treatment-mediated nuclear damage in A549 lung cancer cells. It was demonstrated that untreated (control) cells did not show any significant alterations within the nucleus (Figure 5). On the other hand, EtOH-LCa-treated A549 cells exhibited substantial nuclear condensation and fragmentation. Thus, treatment with EtOH-LCa induces substantial nuclear condensation and fragmentation in A549 lung cancer cells.

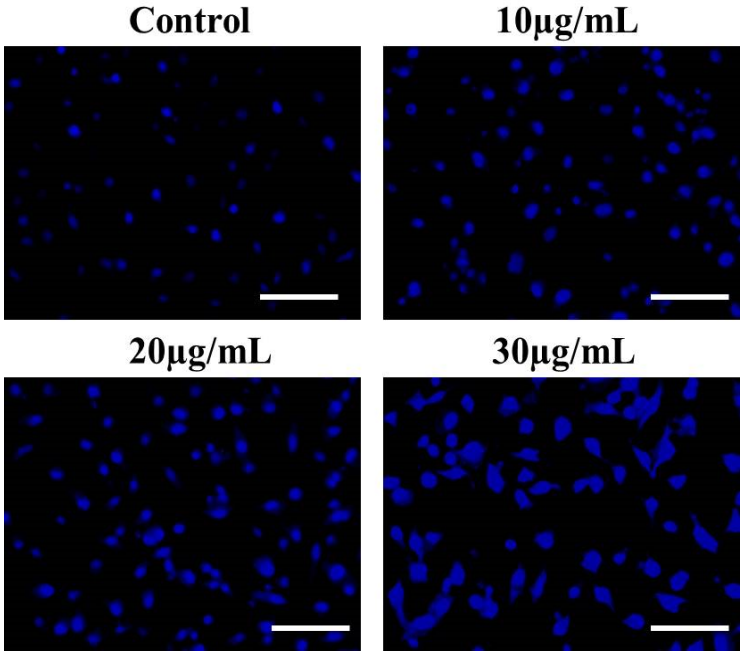

Figure 5. Efficacy of EtOH-LCa in altering the nuclear morphology in A549 cells as studied through DAPI stain. Magnification: 20×; Scale bar = 100 µm.

3.6. Effect of EtOH-LCa on Activation of Caspase-3 in A549 Lung Cancer Cells

Caspases are the primary drivers of apoptotic cell death. Accordingly, we assessed the effect of EtOH-LCa on the activity of caspase-3, which is a downstream effector of caspase. As shown in Figure 6A, treatment of A549 with various concentrations of EtOH-LCa (10 µg/mL, 20 µg/mL and 30 µg/mL) increased the activity of caspase-3 to 33.67 ± 4.26%, 66.12 ± 4.61% and 84.58 ± 4.76%, respectively, as compared to the untreated control.

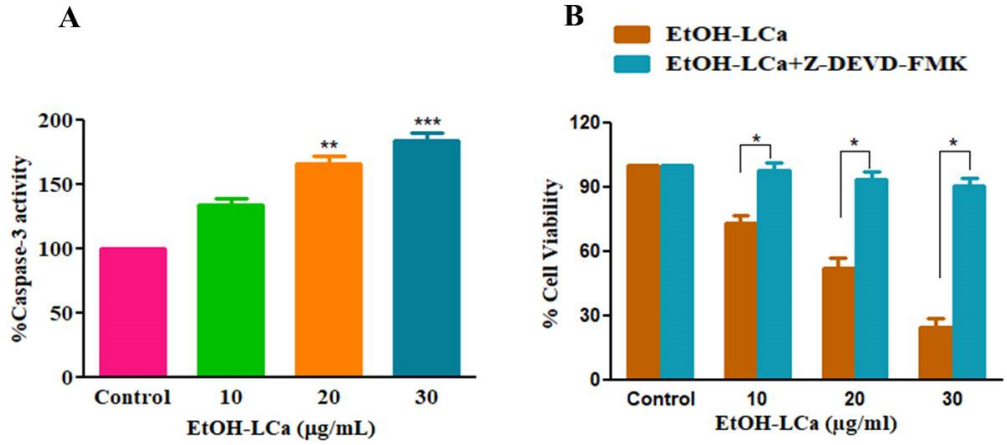

Figure 6. (**A**) Percent (%) caspase-3 activity in A549 cells after treatment with EtOH-LCa. (**B**) Effects of caspase-3 inhibitor pretreatment in ameliorating EtOH-LCa-mediated cytotoxicity within human lung cancer A549 cells. Data represent mean ± SEM. * $p < 0.05$, ** $p < 0.01$ and *** $p < 0.001$.

In addition, and to re-affirm the contribution of caspase-3 to EtOH-LCa-induced apoptosis, A549 cells were pretreated with Z-DEVD-FMK (caspase-3 inhibitor) for 2 h followed by EtOH-LCa treatment. It was demonstrated that pretreatment with caspase-3 inhibitor completely abrogated apoptosis of A549 cells induced by EtOH-LCa (Figure 6B), implicating that apoptosis induced by EtOH-LCa in A549 cells is tightly linked with caspase.

3.7. Effect of EtOH-LCa on Mitochondrial Membrane Potential in Lung Carcinoma Cells

Dissipation of mitochondrial membrane potential (Δψm) impels cytochrome C and apoptosis-inducing factor (AIF) release in the cytoplasm from mitochondria, which are effectual regulators of programmed cell death [22]. We subsequently investigated the effects of EtOH-LCa on mitochondrial membrane potential. As shown in Figure 7, EtOH-LCa treatment decreased mitochondrial membrane potential in a concentration-dependent manner in lung cancer cells. Thus, these findings validate the contribution of mitochondria in EtOH-LCa-induced apoptosis.

3.8. Effect of EtOH-LCa on Expression Levels of Bcl-2 Members in Lung Carcinoma Cells

Previous studies have established that Bcl-2 family proteins are critical for apoptosis induction, mainly via regulating the mitochondrial pathway which is often activated in response to chemotherapeutic drugs [24]. To investigate the underlying mechanism of EtOH-LCa-mediated apoptosis in A549 cancer cells, qRT-PCR analysis was conducted to study the influence of EtOH-LCa treatment on the mRNA expression of Bax, Bad, Bcl-XL, and Bcl-2. It was found that treatment with various concentrations of EtOH-LCa (10 µg/mL, 20 µg/mL and 30 µg/mL) increased the mRNA expression of pro-apoptotic genes Bax and Bad 1.19 ± 0.04, 1.46 ± 0.05 and 1.71 ± 0.06 folds; 1.27 ± 0.04, 1.56 ± 0.05 and 1.81 ± 0.06 folds, respectively, whereas decreased the expression of anti-apoptotic genes Bcl-XL and Bcl-2 to 0.89 ± 0.03, 0.70 ± 0.05 and 0.46 ± 0.03 folds, and 0.78 ± 0.05, 0.65 ± 0.04 and 0.39 ± 0.07 folds, respectively (Figure 8). Hence, we can suggest that EtOH-LCa treatment enhances the expression of pro-apoptotic proteins and decreases the expression of anti-apoptotic proteins.

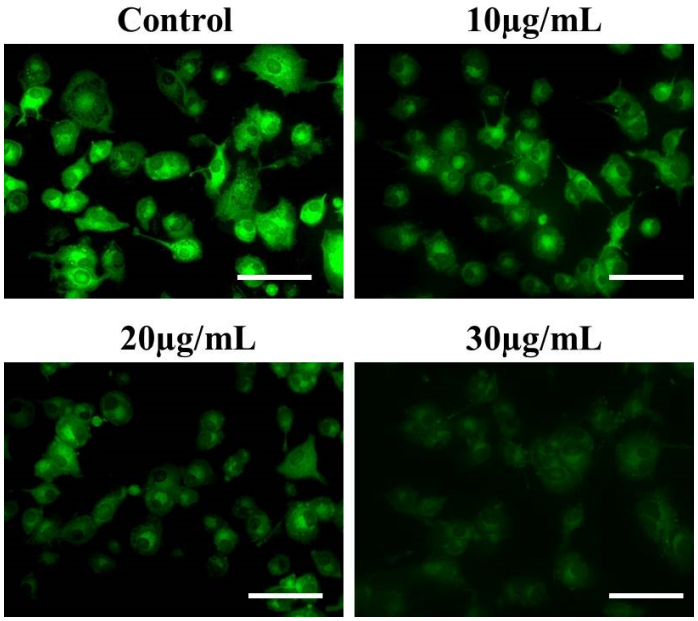

Figure 7. Dissipation of mitochondrial membrane potential (Δψm) in A549 lung cancer cells after treatment with EtOH-LCa as compared to untreated control; Magnification 20×.

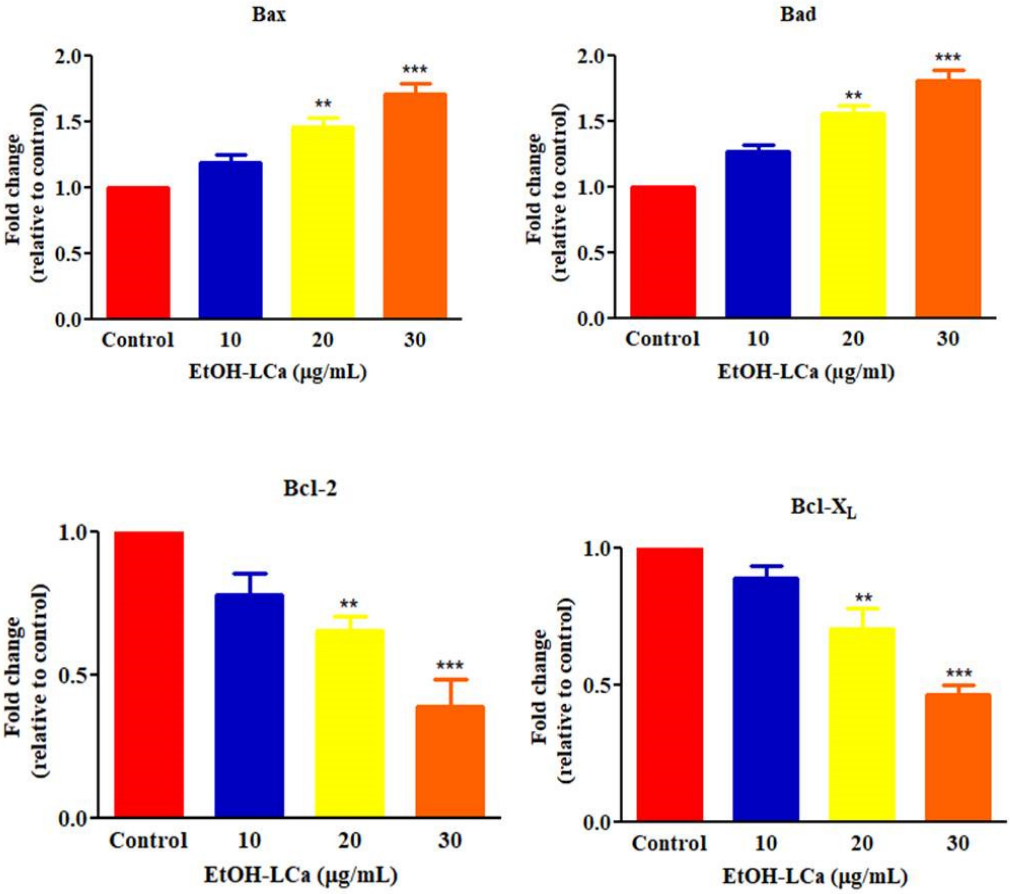

Figure 8. Effect of EtOH-LCa in modulating the gene expression of genes associated with apoptosis; Bax, Bad, Bcl-2, and Bcl-XL. Data represent mean ± SEM. ** $p < 0.01$ and *** $p < 0.001$ vs. untreated control.

3.9. Effect of EtOH-LCa on Cell Cycle Progression of A549 Cells

In order to study whether alterations in the cell cycle distribution were responsible for A549-mediated cell growth inhibition and apoptosis induction, the population of A549 cells in different cell cycle phases was quantified by flow cytometry following treatment with EtOH-LCa. Treatment of A549 cells with 10, 20 and 30 µg/mL EtOH-LCa led to a concentration-dependent accumulation of cells at the G0/G1 phase, compared to untreated cells. The G0/G1percentages were 67.20 ± 3.58% (10 µM), 78.86 ± 4.77% (20 µM), 86.23 ± 4.02% (30 µM), respectively, compared to untreated cells (28.29 ± 3.28%) (Figure 9).

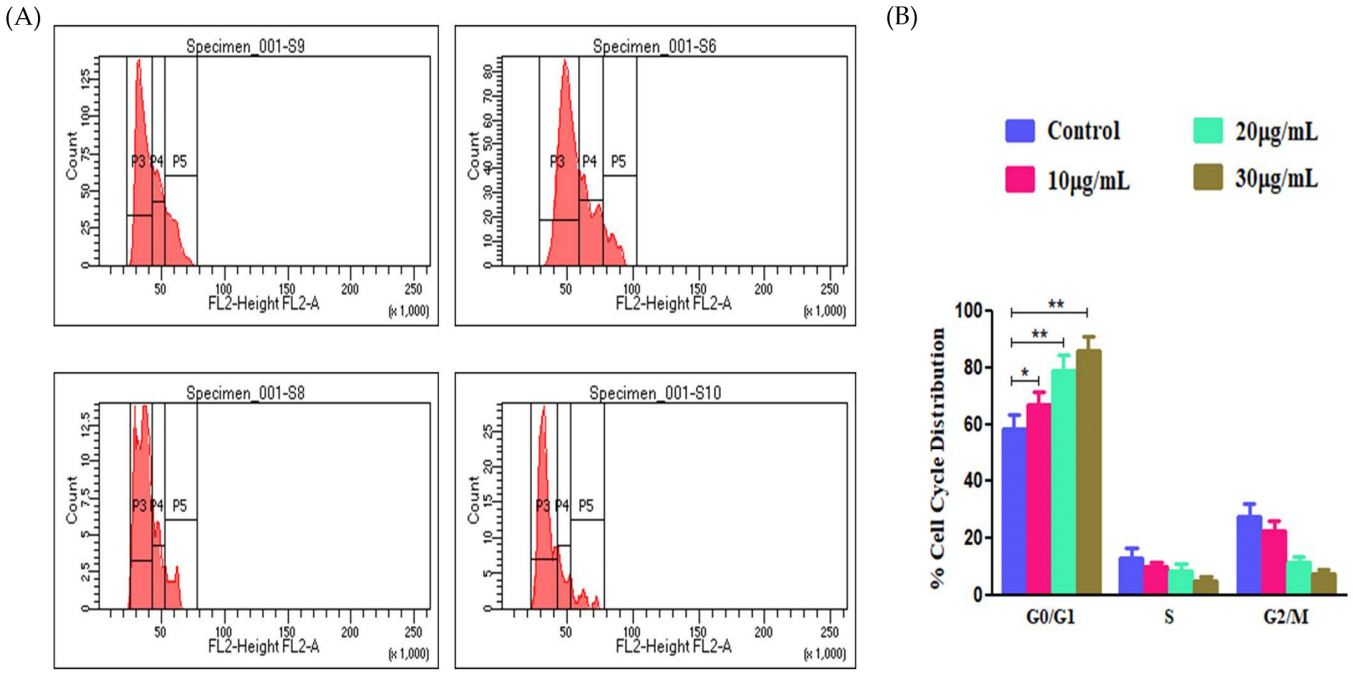

Figure 9. Abrogation of cell cycle progression post-EtOH-LCa treatment within A549 cells. (**A**) Cell cycle distribution of PI-stained A549 cells treated with 10–30µg/mL EtOH-LCa for 24 h observed by flow cytometry, and (**B**) percent (%) cell cycle distribution of cells in different phases of the cell cycle as evaluated during flow cytometry. Data reported includes mean ± SEM of three separate experiments. * $p < 0.05$ and ** $p < 0.01$ vs. untreated control.

3.10. EtOH-LCa Inhibited the NF-kB Signaling Pathway in Lung Carcinoma Cells

The effects of EtOH-LCa treatment on the NF-kB signaling pathway in lung cancer cells were studied using the enzyme-linked immunosorbent assay (ELISA). Our findings revealed that EtOH-LCa at concentrations of 10, 20, and 30 µg/mL significantly reduced the levels of NFκB p65 to 3.67 ± 0.77 ng/mL, 7.45 ± 0.85, and 9.51 ± 0.22, respectively as compared to nontreated A549 cells (Figure 10). Thus, it can be concluded that the treatment with increasing concentrations of EtOH-LCa inhibits the NF-kB signaling pathway in lung cancer cells in a concentration-dependent manner.

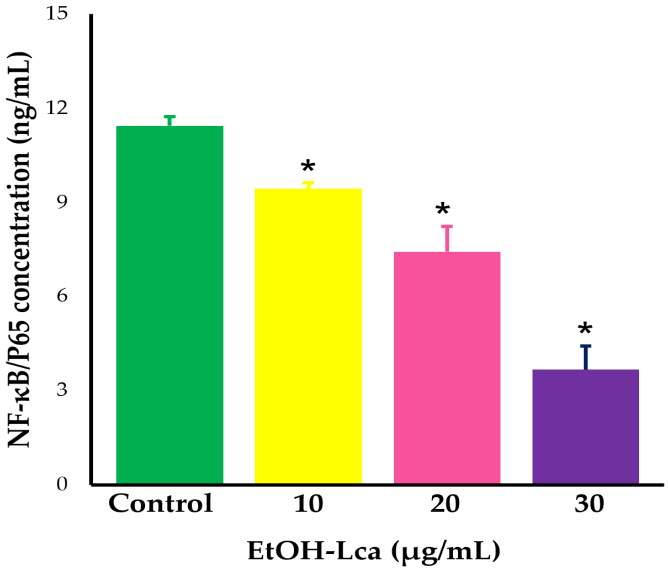

Figure 10. NF-κB/p65 levels in lung cancer cells following treatment with different concentrations of EtOH-LCa. * $p < 0.05$. Data represent mean ± SEM of three separate experiments. * $p < 0.05$ vs. untreated control.

4. Discussion

Recent alterations in the lifestyle of people focusing on low consumption of fruits and vegetables, lack of exercise and excessive consumption of alcohol and smoking have led to increased incidences of lung cancer [25]. Although regular check-ups and screening methods have declined the death rates; the risk of lung cancer is increasing on an annual basis [26,27]. Therefore, there is an intense requirement for the exploration of novel anticancer drug candidates with good efficacy along with less cytotoxic effects on normal cells. This report demonstrates, for the first time, the anticancer and apoptotic efficiency of ethanolic extract of *C. aromaticus* leaves (EtOH-LCa) against lung cancer cells. Our results clearly demonstrated that EtOH-LCa reduced cell viability with increases in active caspase-3 and the Bax to Bcl-2 expression levels in A549 lung cancer cells and with a concomitant decrease in the expression levels of anti-apoptotic genes; Bcl-XL and Bcl-2. Most importantly, EtOH-LCa impeded NF-kB/p65 signaling pathway activation. These findings imply the potential anticancer activity of EtOH-LCa against lung cancer cells.

Apoptosis, also known as programmed cell death, is a natural process that happens as a homeostatic mechanism to preserve cell populations in tissues during development and aging [28,29]. Most importantly, apoptosis acts as an innate defense mechanism in many pathological conditions; particularly cancer, via regulating cell growth and/or division to halt uncontrol cancer cell proliferation [30]. Consequently, the induction of programmed cell death is deemed as a plausible therapeutic target for the clinical management of various types of cancer [31]. Generally, apoptosis is distinguished by DNA fragmentation and/or chromatin condensation, both of which were observed in A549 cells after EtOH-LCa treatment. Moreover, DAPI staining was performed to investigate the alterations in nuclear morphology of EtOH-LCa-treated A549 cells. It was evident that EtOH-LCa treatment mediates the nuclear condensation and fragmentation within the lung cancer cells.

Two distinct biochemical pathways, an intrinsic mitochondrial-dependent pathway and an extrinsic death receptor-dependent mechanism, are mainly involved in the elicitation of programmed cell death. Both pathways involve the activation of a unique family of cysteine proteases; caspases, which in turn, exert a key role in modulating programmed cell death [32]. In this study, EtOH-LCa treatment resulted in a considerable dissipation of mitochondrial membrane potential ($\Delta\psi m$), which was accompanied by a concentration-dependent increase in the activities of caspase-3, with a concomitant induction of apoptosis amongst A549 cancer cells. Interestingly, EtOH-LCa-triggered cytotoxicity was alleviated

in A549 cells that had been pre-exposed to the selective caspase-3 inhibitor, Z-DEVD-FMK. Similar findings were stated by Khafagy et al. [33] who emphasized the contribution of caspase cascade activation to the strong cytotoxic effect of ethanolic extract of *Rubus chingii* leaves against lung cancer cells. Of note, the apoptotic molecular mechanism caused by EtOH-LCa was further studied by examining the changes in mRNA expression of apoptosis-related genes. According to the RT-PCR data, the induction of apoptosis in A549 cells was accompanied by up-regulation of pro-apoptotic genes (Bad and Bax) and downregulation of the anti-apoptotic genes (Bcl-XL and Bcl-2). It has been reported that in response to various forms of cell stress or injury, Bcl-associated X proteins are freed from their link with Bcl-2, resulting in the formation of holes in the mitochondrial membrane, leading to the release of cytochrome C and subsequent caspase pathway activation [34]. Collectively, our findings clearly indicate that EtOH-LCa-triggers apoptosis in A549 cancer cells is mediated, at least in part, via the intrinsic mitochondrial-mediated cell death pathway.

Reactive oxygen species (ROS) are unstable species and considered as the ultimate byproducts of oxidative stress. ROS in cancer cells mediates a crucial role in cell death regulation. A mounting body of evidence has verified the contribution of ROS instigation to the anticancer activities of natural products [35,36]. Furthermore, it is widely understood that the generation of ROS is one of the probable events prompted by the loss of mitochondrial integrity [37,38]. Herein, the role of ROS generation in the cytotoxic effect of EtOH-LCa on A549 cells was investigated. Treatment with EtOH-LCa resulted in an escalation of intracellular ROS levels within A549 cells in a concentration-dependent manner. Our data clearly emphasize the potential of EtOH-LCa in triggering ROS-mediated oxidative stress within A549 lung carcinoma cells, which could participate in the cytotoxic activity of EtOH-LCa against lung cancer cells.

In order to gain more insight into the anti-proliferative efficacy of EtOH-LCa, the distribution of treated cells in various cell cycle phases, namely, the G0/G1, S and G2/M phases, was detected using PI staining. Generally, G0/G1 and G2/M stages of the cell cycle are the major checkpoints and are implicated with critical roles in cell cycle regulation. Our data reveals that EtOH-LCa arrested the progression of the cell cycle at G0/G1 in NSCLC A549 cells by preventing the transition from G0/G1 to S and thus resulting in their apoptosis.

Nuclear factor- κB (NF-κB) is a transcription factor that controls several biological processes, including cell development and survival. NF-κB and its related pathways have been shown to encourage cancer development and progression by promoting angiogenesis and altering the immunological and metabolic status of the tumor microenvironment [39,40]. Moreover, NF-κB activation by chemo- and/or rado-therapy was linked to treatment failure and resistance [41]. Recently, many reports have recognized the correlation between NF-κB and lung carcinogenesis, emphasizing the implication of NF-κB signaling pathway as a promising target for the management of lung cancer [42]. Herein, we found that treatment with EtOH-LCa efficiently lowered the expression of NF-κB/p65 in A549 cancer cells. Conclusively, these findings suggest that EtOH-LCa could halt the growth of lung cancer cells via impeding the NF-kB signaling pathway. Nevertheless, additional studies are required to fully explicate the molecular pathway(s) pertaining to EtOH-LCa-mediated apoptosis in A549 lung cancer cells.

5. Conclusions

To sum up, our report demonstrated that EtOH-LCa holds an excellent apoptotic as well as anticancer potential against lung carcinoma cells. Our results exhibited that the EtOH-LCa-mediated anti-growth effect on A549 lung cancer cells is linked with abrogation of the cell cycle, induction of apoptosis arising from the dissipation of mitochondrial membrane potential, production of ROS, activation of caspases and alteration of gene expression of Bcl2 family members. Most importantly, it was evident that EtOH-LCa exerts its growth-suppressing and apoptotic effects on A549 lung cancer cells probably by the

inhibition of the NF-κB signaling pathway. Collectively, our data provide preliminary evidence of EtOH-LCa as a potential chemo-preventive agent in lung cancer cells.

Author Contributions: Conceptualization, G.S., A.A. (Ahmed Alafnan) and S.M.H.; methodology, G.S., A.A. (Ahmed Alafnan), T.H. and S.M.H.; software, E.-S.K., A.A.K. and A.A. (Abdulwahab Alamri); formal analysis, E.-S.K., A.A.K. and A.A. (Abdulwahab Alamri); investigation, G.S., A.A. (Ahmed Alafnan), T.H. and S.M.H.; resources, G.S.; writing—original draft preparation, G.S. and A.S.A.L.; writing—review and editing, G.S. and A.S.A.L.; supervision, A.A. (Ahmed Alafnan); funding acquisition, G.S. All authors have read and agreed to the published version of the manuscript.

Funding: This research received no external funding.

Data Availability Statement: Not applicable.

Acknowledgments: The authors thank the University of Hail's Deanship of Scientific Research for supporting this research by the awarded grant No. 160971.

Conflicts of Interest: The authors declare no conflict of interest.

References

1. Siegel, R.L.; Miller, K.D.; Fuchs, H.E.; Jemal, A. Cancer Statistics, 2021. *CA Cancer J. Clin.* **2021**, *71*, 7–33. [CrossRef]
2. Aldawsari, M.F.; Alalaiwe, A.; Khafagy, E.S.; Al Saqr, A.; Alshahrani, S.M.; Alsulays, B.B.; Alshehri, S.; Abu Lila, A.S.; Danish Rizvi, S.M.; Hegazy, W.A.H. Efficacy of SPG-ODN 1826 Nanovehicles in Inducing M1 Phenotype through TLR-9 Activation in Murine Alveolar J774A.1 Cells: Plausible Nano-Immunotherapy for Lung Carcinoma. *Int. J. Mol. Sci.* **2021**, *22*, 6833. [CrossRef]
3. Subaiea, G.M.; Rizvi, S.M.D.; Yadav, H.K.S.; Al Hagbani, T.; Abdallah, M.H.; Khafagy, E.-S.; Gangadharappa, H.V.; Hussain, T.; Abu Lila, A.S. Ganetespib with Methotrexate Acts Synergistically to Impede NF-κB/p65 Signaling in Human Lung Cancer A549 Cells. *Pharmaceuticals* **2023**, *16*, 230. [CrossRef]
4. Rockswold, G.L.; Ramsey, H.E.; Buker, G.D. The results of treatment of lung cancer by surgery, radiation and chemotherapy at a USPHS hospital. *Mil. Med.* **1970**, *135*, 362–368. [CrossRef]
5. Deng, L.J.; Qi, M.; Li, N.; Lei, Y.H.; Zhang, D.M.; Chen, J.X. Natural products and their derivatives: Promising modulators of tumor immunotherapy. *J. Leukoc. Biol.* **2020**, *108*, 493–508. [CrossRef]
6. Bernstein, N.; Akram, M.; Yaniv-Bachrach, Z.; Daniyal, M. Is it safe to consume traditional medicinal plants during pregnancy? *Phytother. Res.* **2020**, *35*, 1908–1924. [CrossRef]
7. Cragg, G.M.; Newman, D.J. Plants as a source of anti-cancer agents. *J. Ethnopharmacol.* **2005**, *100*, 72–79. [CrossRef]
8. Jimmy, J.L. Coleus aromaticus Benth.: An update on its bioactive constituents and medicinal properties. *All. Life* **2021**, *14*, 756–773. [CrossRef]
9. Wadikar, D.D.; Patki, P.E. Coleus aromaticus: A therapeutic herb with multiple potentials. *J. Food Sci. Technol.* **2016**, *53*, 2895–2901. [CrossRef]
10. Hariram, N. Coleus aromaticus Benth Synthesis of Potentially Nanomedicine as High Nutritive Value of Human Health and Immunomodulator. *IJSRM* **2016**, *4*, 18–38.
11. Khare, R.S.; Kundu, S. Coleus Aromaticus Benth—A Nutritive Medicinal Plant Of Potential Therapeutic Value. *Int. J. Pharma Bio Sci.* **2011**, *2*, 488–500.
12. Rai, V.M.; Pai, V.R.; Kedilaya, P. A preliminary evaluation of anticancer and antioxidant potential of two traditional medicinal plants from Lamiaceae—Pogostemon heyneanus and Plectranthus amboinicus. *J. Appl. Pharm. Sci.* **2016**, *6*, 073–078. [CrossRef]
13. Yulianto, W.; Andarwulan, N.; Giriwono, P.E.; Pamungkas, J. HPLC-based metabolomics to identify cytotoxic compounds from Plectranthus amboinicus (Lour.) Spreng against human breast cancer MCF-7Cells. *J. Chromatogr. B Anal. Technol. Biomed. Life Sci.* **2016**, *1039*, 28–34. [CrossRef]
14. Baldwin, A.S., Jr. The NF-kappa B and I kappa B proteins: New discoveries and insights. *Annu. Rev. Immunol.* **1996**, *14*, 649–683. [CrossRef]
15. Karin, M.; Lin, A. NF-kappaB at the crossroads of life and death. *Nat. Immunol.* **2002**, *3*, 221–227. [CrossRef]
16. Chen, W.; Li, Z.; Bai, L.; Lin, Y. NF-kappaB in lung cancer, a carcinogenesis mediator and a prevention and therapy target. *Front. Biosci. (Landmark Ed.)* **2011**, *16*, 1172–1185. [CrossRef]
17. Wang, X.; Chen, W.; Lin, Y. Sensitization of TNF-induced cytotoxicity in lung cancer cells by concurrent suppression of the NF-kappaB and Akt pathways. *Biochem. Biophys. Res. Commun.* **2007**, *355*, 807–812. [CrossRef]
18. Wang, X.; Ju, W.; Renouard, J.; Aden, J.; Belinsky, S.A.; Lin, Y. 17-allylamino-17-demethoxygeldanamycin synergistically potentiates tumor necrosis factor-induced lung cancer cell death by blocking the nuclear factor-kappaB pathway. *Cancer Res.* **2006**, *66*, 1089–1095. [CrossRef]
19. Gyrd-Hansen, M.; Meier, P. IAPs: From caspase inhibitors to modulators of NF-kappaB, inflammation and cancer. *Nat. Rev. Cancer* **2010**, *10*, 561–574. [CrossRef]

20. Kani, K.; Momota, Y.; Harada, M.; Yamamura, Y.; Aota, K.; Yamanoi, T.; Takano, H.; Motegi, K.; Azuma, M. γ-tocotrienol enhances the chemosensitivity of human oral cancer cells to docetaxel through the downregulation of the expression of NF-κB-regulated anti-apoptotic gene products. *Int. J. Oncol.* **2013**, *42*, 75–82. [CrossRef]
21. Alshehri, A.; Ahmad, A.; Tiwari, R.K.; Ahmad, I.; Alkhathami, A.G.; Alshahrani, M.Y.; Asiri, M.A.; Almeleebia, T.M.; Saeed, M.; Yadav, D.K.; et al. In Vitro Evaluation of Antioxidant, Anticancer, and Anti-Inflammatory Activities of Ethanolic Leaf Extract of Adenium obesum. *Front. Pharmacol.* **2022**, *13*, 847534. [CrossRef]
22. Ahmad, A.; Tiwari, R.K.; Mishra, P.; Alkhathami, A.G.; Almeleebia, T.M.; Alshahrani, M.Y.; Ahmad, I.; Asiri, R.A.; Alabdullah, N.M.; Hussien, M.; et al. Antiproliferative and apoptotic potential of Glycyrrhizin against HPV16+ Caski cervical cancer cells: A plausible association with downreguation of HPV E6 and E7 oncogenes and Notch signaling pathway. *Saudi J. Biol. Sci.* **2022**, *29*, 3264–3275. [CrossRef]
23. Ahmad, A.; Ansari, I.A. Carvacrol Exhibits Chemopreventive Potential against Cervical Cancer Cells via Caspase-Dependent Apoptosis and Abrogation of Cell Cycle Progression. *Anti-Cancer Agents Med. Chem.* **2021**, *21*, 2224–2235. [CrossRef]
24. Ahmad, A.; Tiwari, R.K.; Saeed, M.; Al-Amrah, H.; Han, I.; Choi, E.H.; Yadav, D.K.; Ansari, I.A. Carvacrol instigates intrinsic and extrinsic apoptosis with abrogation of cell cycle progression in cervical cancer cells: Inhibition of Hedgehog/GLI signaling cascade. *Front. Chem.* **2023**, *10*, 1064191. [CrossRef]
25. Khaltaev, N.; Axelrod, S. Global lung cancer mortality trends and lifestyle modifications: Preliminary analysis. *Chin. Med. J.* **2020**, *133*, 1526–1532. [CrossRef]
26. Bruder, C.; Bulliard, J.L.; Germann, S.; Konzelmann, I.; Bochud, M.; Leyvraz, M.; Chiolero, A. Estimating lifetime and 10-year risk of lung cancer. *Prev. Med. Rep.* **2018**, *11*, 125–130. [CrossRef]
27. Elmore, S. Apoptosis: A review of programmed cell death. *Toxicol. Pathol.* **2007**, *35*, 495–516. [CrossRef]
28. Lila, A.S.; Kiwada, H.; Ishida, T. Selective delivery of oxaliplatin to tumor tissue by nanocarrier system enhances overall therapeutic efficacy of the encapsulated oxaliplatin. *Biol. Pharm. Bull.* **2014**, *37*, 206–211. [CrossRef]
29. Chaudhry, G.E.; Md Akim, A.; Sung, Y.Y.; Sifzizul, T.M.T. Cancer and apoptosis: The apoptotic activity of plant and marine natural products and their potential as targeted cancer therapeutics. *Front. Pharm.* **2022**, *13*, 842376. [CrossRef]
30. Pfeffer, C.M.; Singh, A.T.K. Apoptosis: A Target for Anticancer Therapy. *Int. J. Mol. Sci.* **2018**, *19*, 448. [CrossRef]
31. Wen, X.; Lin, Z.Q.; Liu, B.; Wei, Y.Q. Caspase-mediated programmed cell death pathways as potential therapeutic targets in cancer. *Cell. Prolif.* **2012**, *45*, 217–224. [CrossRef]
32. Khafagy, E.-S.; Al Saqr, A.; Alotaibi, H.F.; Abu Lila, A.S. Cytotoxic and Apoptotic Effect of Rubus chingii Leaf Extract against Non-Small Cell Lung Carcinoma A549 Cells. *Processes* **2022**, *10*, 1537. [CrossRef]
33. Brunelle, J.K.; Letai, A. Control of mitochondrial apoptosis by the Bcl-2 family. *J. Cell. Sci.* **2009**, *122*, 437–441. [CrossRef]
34. Al Saqr, A.; Khafagy, E.S.; Aldawsari, M.F.; Almansour, K.; Abu Lila, A.S. Screening of Apoptosis Pathway-Mediated Anti-Proliferative Activity of the Phytochemical Compound Furanodienone against Human Non-Small Lung Cancer A-549 Cells. *Life* **2022**, *12*, 114. [CrossRef]
35. Khan, A.Q.; Rashid, K.; AlAmodi, A.A.; Agha, M.V.; Akhtar, S.; Hakeem, I.; Raza, S.S.; Uddin, S. Reactive oxygen species (ROS) in cancer pathogenesis and therapy: An update on the role of ROS in anticancer action of benzophenanthridine alkaloids. *Biomed. Pharm.* **2021**, *143*, 112142. [CrossRef]
36. Marchi, S.; Giorgi, C.; Suski, J.M.; Agnoletto, C.; Bononi, A.; Bonora, M.; De Marchi, E.; Missiroli, S.; Patergnani, S.; Poletti, F.; et al. Mitochondria-ros crosstalk in the control of cell death and aging. *J. Signal. Transduct.* **2012**, *2012*, 329635. [CrossRef]
37. Zorov, D.B.; Juhaszova, M.; Sollott, S.J. Mitochondrial reactive oxygen species (ROS) and ROS-induced ROS release. *Physiol. Rev.* **2014**, *94*, 909–950. [CrossRef]
38. O'Neil, B.H.; Funkhouser, W.K.; Calvo, B.F.; Meyers, M.O.; Kim, H.J.; Goldberg, R.M.; Bernard, S.A.; Caskey, L.; Deal, A.M.; Wright, F.; et al. Nuclear factor κ-light chain-enhancer of activated B cells is activated by radiotherapy and is prognostic for overall survival in patients with rectal cancer treated with preoperative fluorouracil-based chemoradiotheraphy. *Int. J. Radiat. Oncol. Biol. Phys.* **2011**, *80*, 705–711. [CrossRef]
39. Hoesel, B.; Schmid, J.A. The complexity of NF-κB signaling in inflammation and cancer. *Mol. Cancer* **2013**, *12*, 86. [CrossRef]
40. Liu, Y.P.; Zheng, C.C.; Huang, Y.N.; He, M.L.; Xu, W.W.; Li, B. Molecular mechanisms of chemo- and radiotherapy resistance and the potential implications for cancer treatment. *MedComm* **2021**, *2*, 315–340. [CrossRef]
41. Rasmi, R.R.; Sakthivel, K.M.; Guruvayoorappan, C. NF-κB inhibitors in treatment and prevention of lung cancer. *Biomed. Pharmacother.* **2020**, *130*, 110569. [CrossRef]
42. Cai, Z.; Tchou-Wong, K.-M.; Rom, W.N. NF-kappaB in Lung Tumorigenesis. *Cancers* **2011**, *3*, 4258–4268. [CrossRef]